doi:10.1038/nature10600

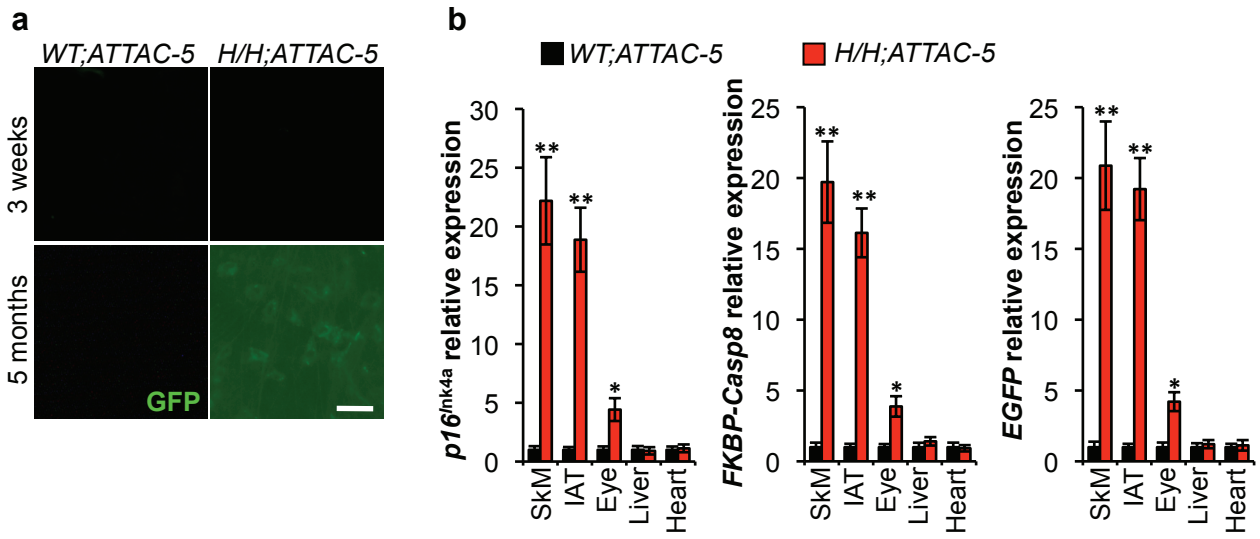

Supplementary Fig. 1: Validation of *p16*^{Ink4a}-specific expression of the *INK-ATTAC-5 transgene.* **a**, GFP intensity of IAT collected from 3-week and 5-month-old untreated mice with the indicated genotypes. Scale bar, 20 μm. **b**, qRT-PCR analysis of untreated 10-month-old mouse tissue analyzed for the relative expression of *p16*^{Ink4a}, *FKBP-Casp8*, and *EGFP*. Error bars, s.d.; *n* = 3 female mice per genotype. **P < 0.05, **P < 0.01*.

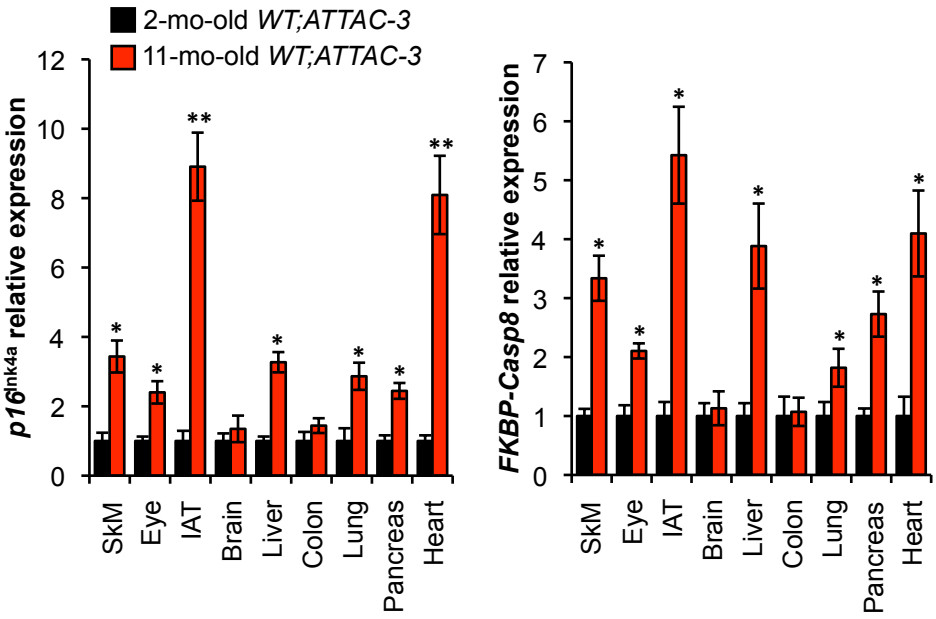

Supplementary Fig. 2: *p16*^{Ink4a} and *INK-ATTAC* expression concurrently increase with chronological aging. Analysis of *p16*^{Ink4a} and *INK-ATTAC* expression in various tissues of 2- and 11-month-old *WT;INK-ATTAC* mice. Error bars, s.d.; *n* = 3 females per age group. **P < 0.05, **P < 0.01.*

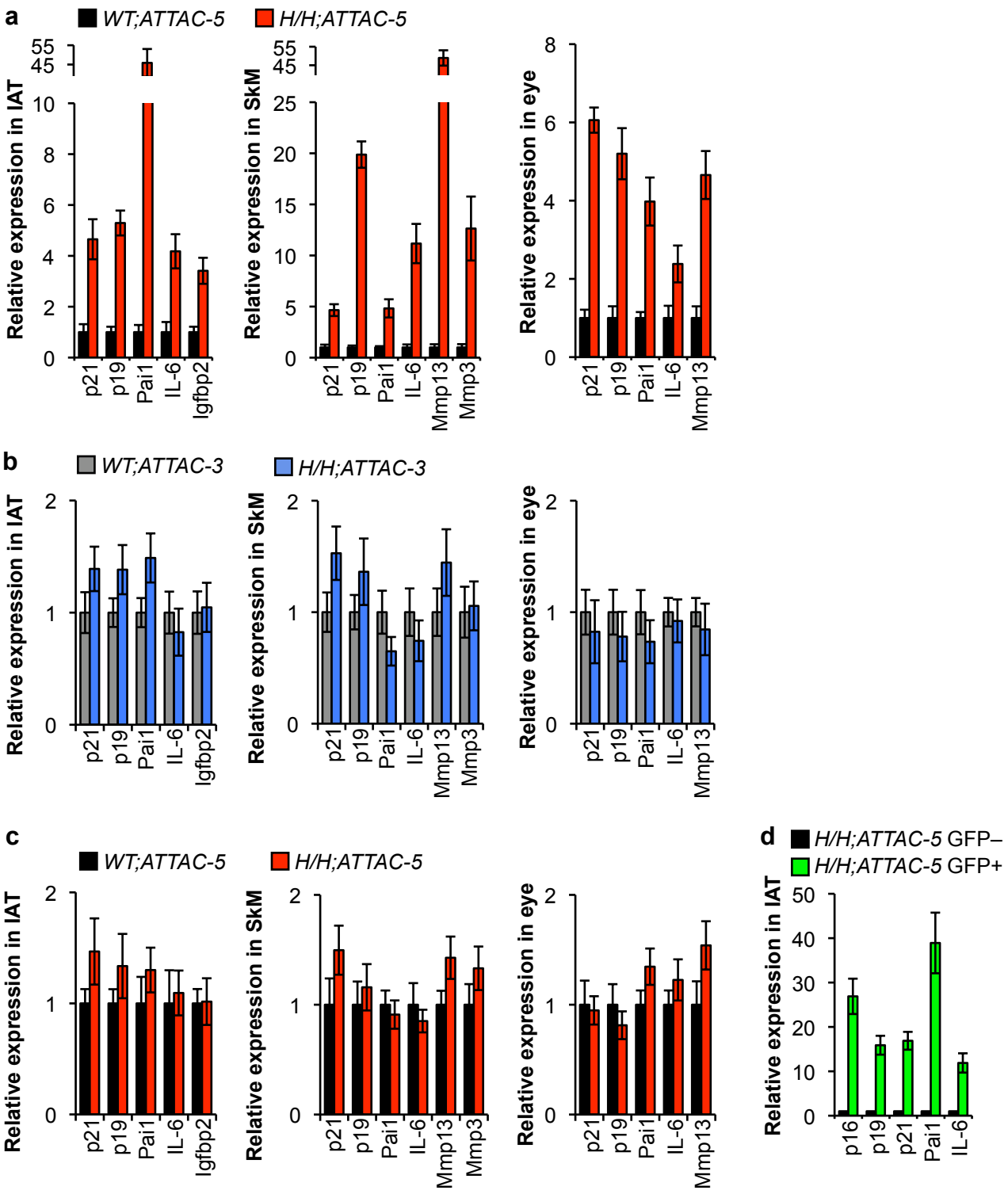

Supplementary Fig. 3: Tissues expressing the *INK-ATTAC-5* transgene display elevated indicators of senescence. a, Relative expression of senescence markers in the indicated tissues of 10-month-old *BubR1*$^{H/H}$*;INK-ATTAC-5* and *WT;INK-ATTAC-5* mice as measured by qRT-PCR. All increases are statistically significant ($P < 0.05$). **b**, Relative expression of senescence markers in the indicated tissues of 3-week-old *WT;INK-ATTAC-3* and *BubR1*$^{H/H}$*;INK-ATTAC-3* mice as measured by qRT-PCR. There were no significant differences. **c**, As in **b** but for 3-week-old *WT;INK-ATTAC-5* and *BubR1*$^{H/H}$*;INK-ATTAC-5* mice. **d**, GFP^{+} and GFP^{-} cell populations from IAT of 10-month-old *BubR1*$^{H/H}$*;INK-ATTAC-5* mice analyzed for relative expression of various senescence markers by qRT-PCR. All increases are statistically significant ($P < 0.01$). Error bars, s.d.; n = 3 female mice per genotype

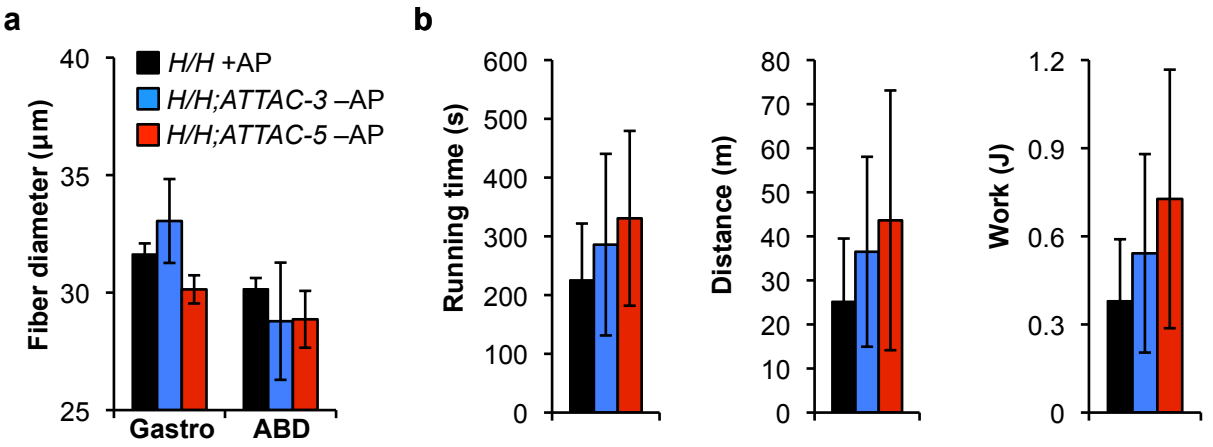

c

Mouse (treatment)	Weight (g)	Fat (%)	POV (g)	Peri (g)	IAT (g)	Mes (g)	SSAT (g)	Brown (g)
H/H (+AP)	18.2 (2.9)	16.1 (1.9)	0.100 (0.04)	0.011 (0.003)	0.068 (0.03)	0.078 (0.01)	0.060 (0.01)	0.095 (0.016)
H/H;ATTAC-3 (–AP)	17.4 (1.8)	15.6 (3.4)	0.054 (0.05)	0.016 (0.02)	0.058 (0.02)	0.063 (0.05)	0.038 (0.01)	0.084 (0.005)
H/H;ATTAC-5 (–AP)	16.7 (2.2)	15.4 (2.5)	0.137 (0.13)	0.020 (0.01)	0.075 (0.05)	0.061 (0.04)	0.050 (0.02)	0.104 (0.030)

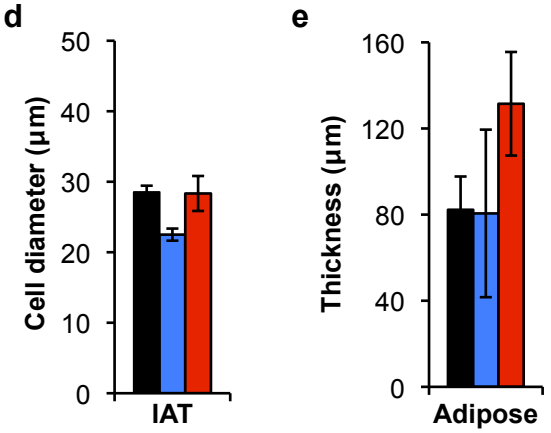

Supplementary Fig. 4: AP20187 treatment of *BubR1*$^{H/H}$ mice does not delay *p16*^{Ink4a}-mediated age-related phenotypes in the absence of *INK-ATTAC*. **a**, Mean muscle fiber diameters of gastrocnemius and abdominal muscles of 10-month-old AP20187-treated *BubR1*$^{H/H}$ mice and non-treated *BubR1*$^{H/H}$;*INK-ATTAC* mice. **b**, Exercise ability of 10-month-old AP20187-treated *BubR1*$^{H/H}$ mice and non-treated *BubR1*$^{H/H}$;*INK-ATTAC* mice. **c**, Body and fat depot weights of 10-month-old AP20187-treated *BubR1*$^{H/H}$ mice and non-treated *BubR1*$^{H/H}$;*INK-ATTAC* mice. Parentheses, s.d. **d**, Mean fat cell diameters in IAT of 10-month-old AP20187-treated *BubR1*$^{H/H}$ and untreated *BubR1*$^{H/H}$;*INK-ATTAC* mice. **e**, Subcutaneous adipose layer thickness of 10-month-old AP20187-treated and untreated *BubR1*$^{H/H}$;*INK-ATTAC* mice. Color codes in **b**, **d** and **e** are as indicated in **a**. Error bars indicate s.e.m. in **a**, **d** and **e**, and s.d. in **b**. For all analyses *n* = 6 female mice per genotype.

a

Genotype (treatment)	BPM (SD)	Sinus pauses % (SD)
WT;ATTAC-3 (–AP) n=3	485.3 (24.7)	0.024 (0.005)
H/H;ATTAC-3 (–AP) n=6	482.5 (35.2)	2.237 (0.135)
H/H;ATTAC-3 (+AP) n=6	456.7 (38.3)	2.176 (0.161)
WT;ATTAC-5 (–AP) n=3	480.8 (29.3)	0.021 (0.004)
H/H;ATTAC-5 (–AP) n=6	466.7 (31.3)	2.124 (0.221)
H/H;ATTAC-5 (+AP) n=6	475.2 (33.9)	2.046 (0.169)

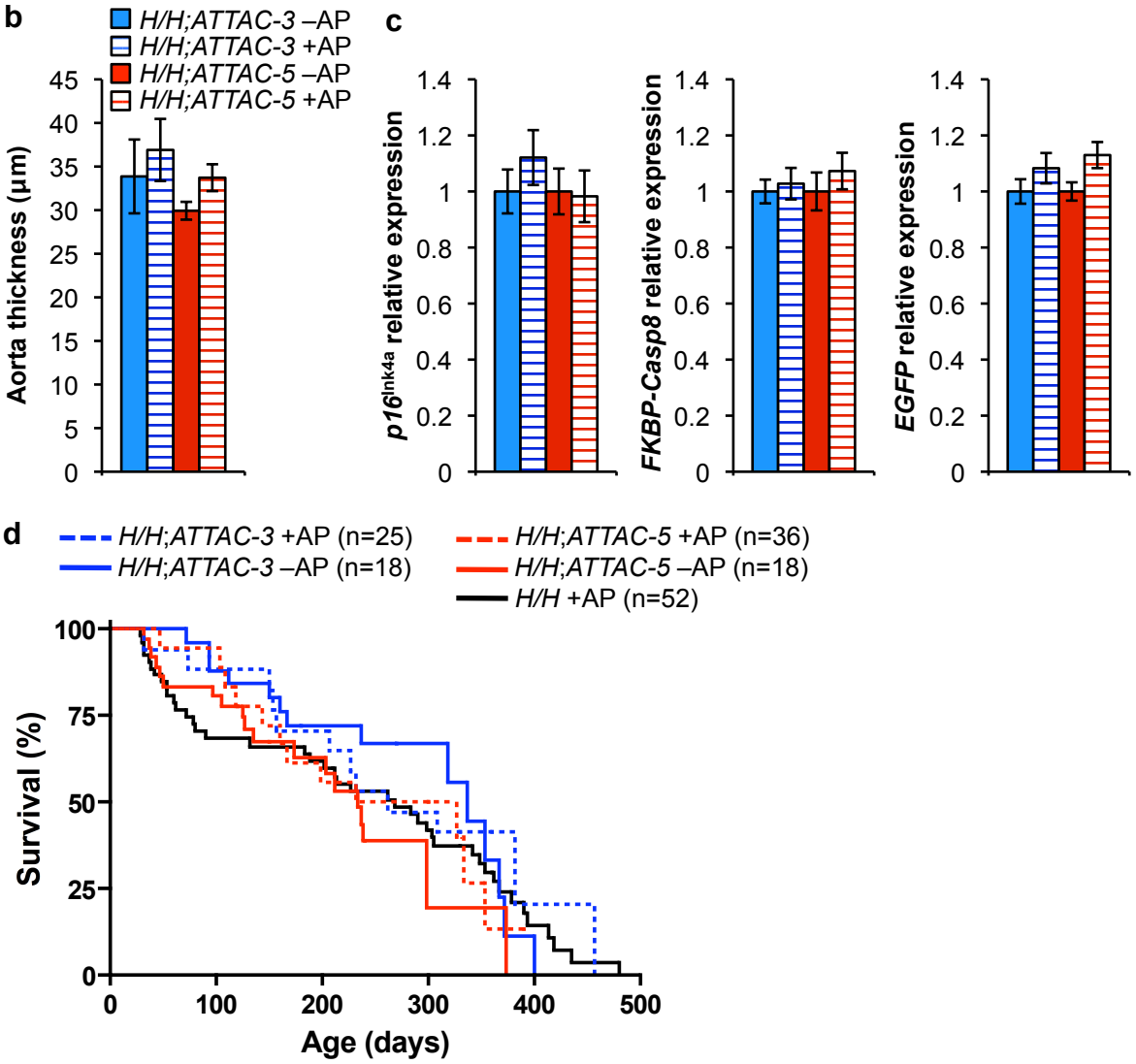

Supplementary Fig. 5: Age-associated traits of BubR1 hypomorphic mice that are *p16*^{Ink4a}-independent are not influenced by clearance of *p16*^{Ink4a}-positive cells. a, Measurement of heart sinus pause rhythm disturbances in mice of the indicated genotypes and treatments. Abbreviation: BPM, beats per min. **b**, Thinning of the aorta is not corrected by drug treatment in *BubR1*$^{H/H}$*;INK-ATTAC* animals. Error bars, s.e.m.; *n* = 6 female mice per genotype. **c**, qRT-PCR analysis of *p16*^{Ink4a} and *INK-ATTAC* expression in aortas of the indicated mice. Error bars, s.d.; *n* = 3 female mice per genotype per treatment. **d**, Survival curves of AP20187-treated and untreated *BubR1*$^{H/H}$*;INK-ATTAC* and AP-treated *BubR1*$^{H/H}$ mice. We note that cardiac stress tests performed on *BubR1*$^{H/H}$ mice indicate that cardiac failure is likely to be the primary cause of death of these animals.

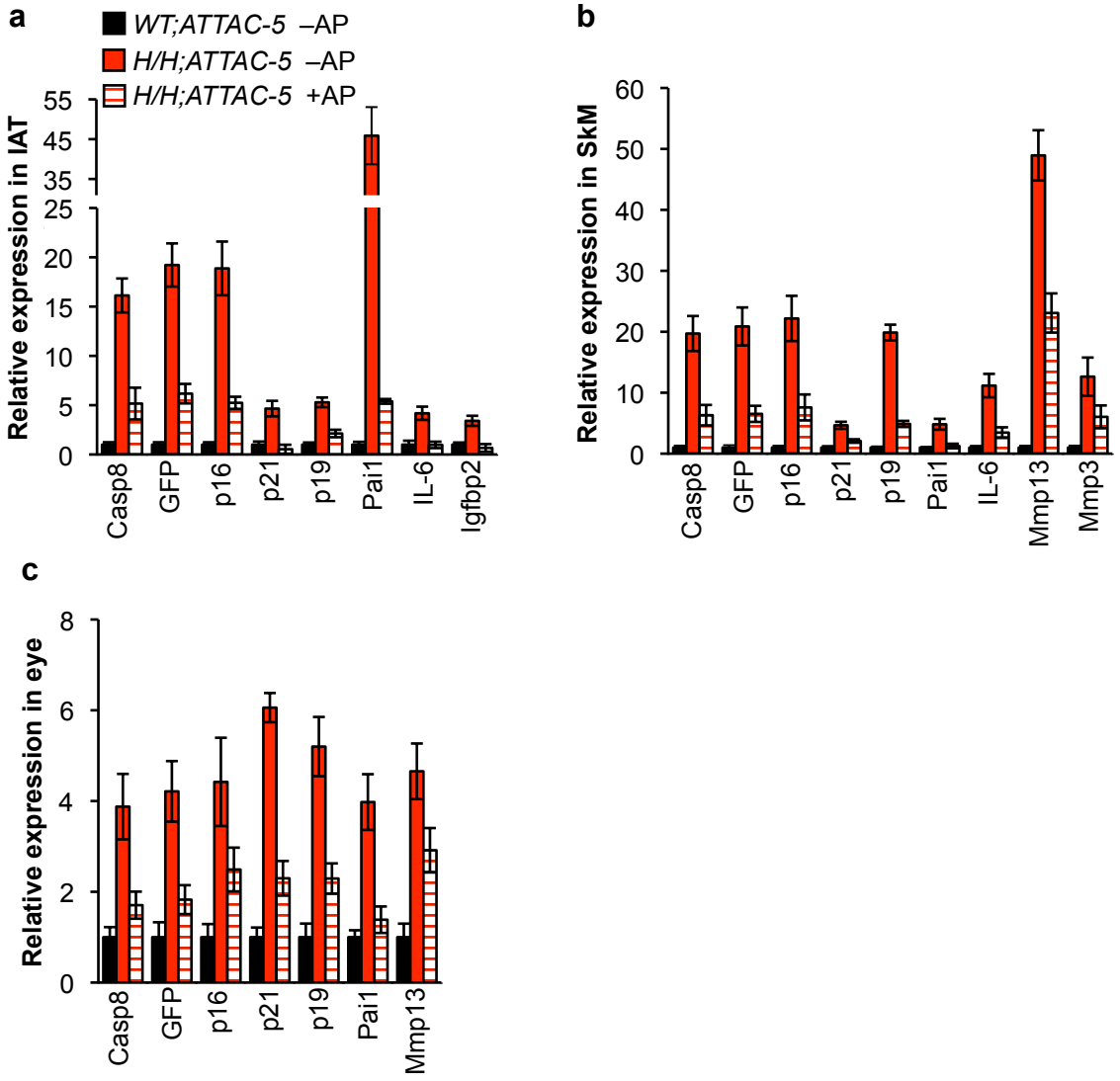

Supplementary Fig. 6: AP20187 treatment of *BubR1*$^{H/H}$*;INK-ATTAC-5* animals reduces p16^{Ink4a}-positive senescent cells. qRT-PCR analysis for indicators of senescence in IAT (**a**), skeletal muscle (gastrocnemius), (**b**) and eye (**c**) reveals that treatment of animals with AP20187 leads to lower levels of senescence-associated markers. Error bars, s.d.; *n* = 3 female mice per genotype. All genes have a significant decrease upon AP20187 treatment (*P* < *0.05*).

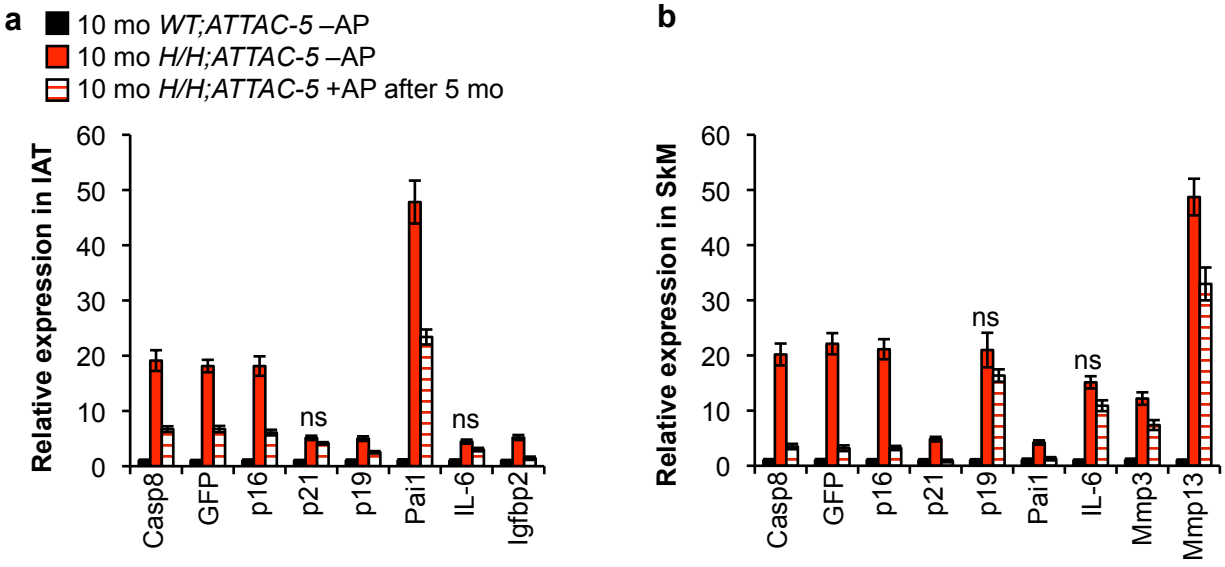

Supplementary Fig. 7: Late-life treatment of *BubR1*$^{H/H}$*;INK-ATTAC-5 animals reduces p16*^{Ink4a}-positive senescent cells. qRT-PCR analysis for indicators of senescence in IAT (**a**) and skeletal muscle (gastrocnemius) (**b)** reveals that treatment of animals with AP20187 leads to lower levels of senescence-associated markers. Error bars, s.d.; *n* = 3 female mice per genotype. All genes (except those marked with ns) have a significant decrease upon AP20187 treatment (*P* < *0.05*).